30th NENE 2021
September 6 - 9
BLED-SLOVENIA
International Conference Nuclear Energy for New Europe

Large interface tracking algorithm for air-water slug in turbulent flow

Jan Kren[1, 2], **Blaž Mikuž**[1]
[1]Reactor Engineering Division
Jožef Stefan Institute
Jamova cesta 39
1000 Ljubljana, Slovenia
jan.kren@ijs.si, blaz.mikuz@ijs.si

[2]University of Ljubljana
Kongresni trg 12
1000 Ljubljana, Slovenia

ABSTRACT

Two-phase flows play an important role in many applications of nuclear power systems. In the two-phase flow experiments large amount of data is usually generated that needs to be classified. One of the first steps is to differentiate between liquid and gas phase with the application of post-processing algorithms.

We are particularly interested in the application of large interface tracking algorithms to Particle Image Velocimetry (PIV) measurements, which have been obtained with high-speed camera in vertical pipe. In such geometry, the reflected light from air-water interface is deformed by refraction through different materials, which results in a low signal-to-noise ratio. Thus, dynamic mask that distinguishes between air and liquid water phase with tracer particles has great importance for the quality of the PIV measurements.

In this paper, we developed two algorithms, which are able to track the large interface of the gas phase in turbulent background flow in PIV-LIF images. The algorithms were developed and tested on different datasets with different bubble lengths, resolutions and seeding density. Algorithms successfully determine the position of the bubble trailing edge and nose, but have a difficulty determining the correct bubble shape.

1 INTRODUCTION

Accurately predicting the behavior of multiphase flows is a problem of immense industrial and scientific interest. Large majority of industrial applications of fluids involve a multiphase flow of one sort or another. In most of these applications, one phase is liquid and the other is gas. In nuclear systems for example the preferential mode of heat transfer is heat transfer by boiling. Two-phase flow is also present during postulated Loss Of Coolant Accident (LOCA), when the system is depressurized and the coolant boils.

A Taylor bubble is an occurence of a slug flow in a vertical pipe. It occupies almost the entire pipe's cross section. These bubbles can be observed in numerous applications in industrial processes including nuclear power plants and are a convenient benchmark case to study bubble coalescence and break-up. Thus, the behaviour of Taylor bubble flows has been

extensively studied in the past decades. An overview of experimental and numerical studies of Taylor bubble flows is given by [1].

Recent high-fidelity numerical simulations [3, 7] showed that a Taylor bubble disintegrates (i.e. decays in size) when it is exposed to turbulent flow regime. It turned out that an accurate prediction of the disintegration rate is particularly challenging in such cases. For that reason, it is necessary to verify the Taylor bubble behavior with an experimental data. Such measurements have been performed for a Taylor bubble in a laminar flow [2] as well as in turbulent flow conditions [5].

Current experimental campaign is focused on determination of velocity fields with Particle Image Velocimetry (PIV) method coupled with Laser Induced Fluorescence (LIF) [8]. In the present study, we have developed algorithms for recognition and tracking of large interfaces in the PIV-LIF images of Taylor bubbles, which is a prerequisite for obtaining the averaged velocity fields around the bubble. Two objectives have been addressed in the present study: (a) development of a simple algorithm for tracking the steamwise position of the Taylor bubble in the pipe and (b) reconstruction of the fluctuating Taylor bubble shape in the turbulent background flow.

2 EXPERIMENT

In our experimental setup (see Figure 1) the Taylor bubble is studied in a counter-current flow regime, where the liquid water flow balances the bouyancy of the Taylor bubble. As a consequence the Taylor bubble can be at approximately constant position for very long periods of time and therefore can be easily studied. The flow rate is measured with Coriolis flow meter. Analytical expression for the velocity of the bubble rise was provided by Dumitrescu [4] and is only a function of the pipe diameter:

$$U_{TB} = 0.35\sqrt{gD} \tag{1}$$

The liquid counter-current is expected to be close to this velocity so that the Taylor bubble is stagnant.
One of the objectives while constructing new experimental device was also ability to study the bubble behavior in pipes with different diameters, which correspond to various flow conditions, e.g. Reynolds, Eötvös and Froude number. Hence, the test section consist of a modular part, which allow separate measurement of a Taylor bubble for various conditions. Current experiments were performed in circular pipe with diameter of $26\,mm$. A constant temperature in the experiment was ensured using a heat exchanger and was measured with two thermometers.

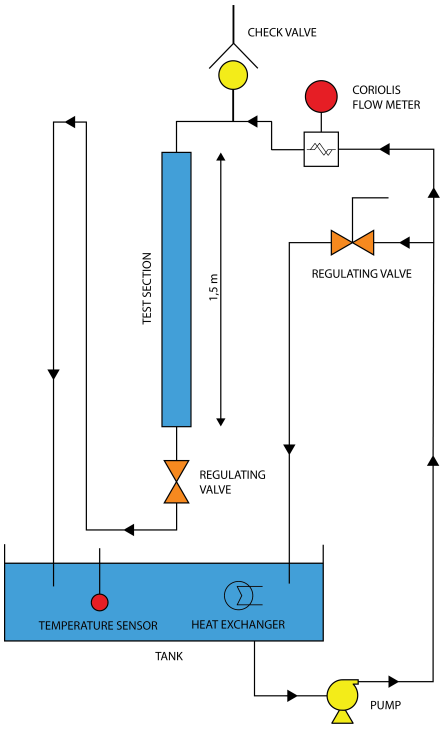

Figure 1: Scheme of the experimental device.

2.1 PIV-LIF method

Velocity fields were measured using PIV-LIF method. PIV is currently the most used optical method for flow visualisation. It is used to obtain instantenous velocity measurements and related flow properties. In our case, the fluid was seeded with small fluorescent tracer particles which follow the flow dynamics. The particles are illuminated with strong laser sheet as seen in Figure 2. As the fluorescent particles emit light of the wavelength between $580 - 610\,nm$ the special filter is added to the camera lens which transmits light of only such wavelength.

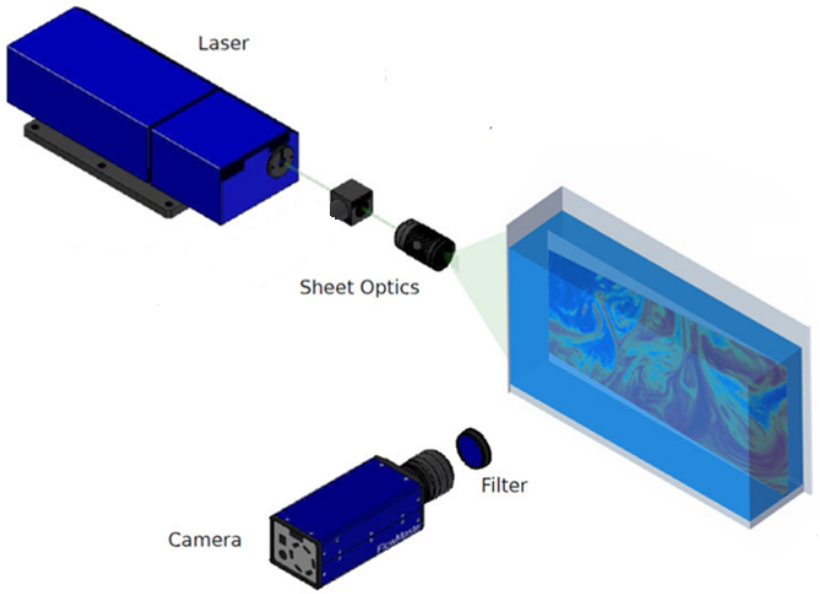

Figure 2: Particle Image Velocimetry with Laser Induced Fluorescence [6].

3 INTERFACE TRACKING ALGORITHM

In Figure 3 a PIV-LIF image of a Taylor bubble is shown. We observe point-like high luminosity at the positions of seeding particles in the liquid phase and large empty space in the middle of the image, which corresponds to the Taylor bubble. Even human eye hardly recognizes the bubble boundaries accurately, but the positions of bubble nose and trailing edge regions can be well defined. Images were taken with the frequency of 200Hz over 2 minutes of time. During this time the bubble fluctuates due to velocity fluctuations in a turbulent background flow. Thus, the bubble shape has to be tracked at several occasions in time. This is a rather time consuming work that needs to be automated.

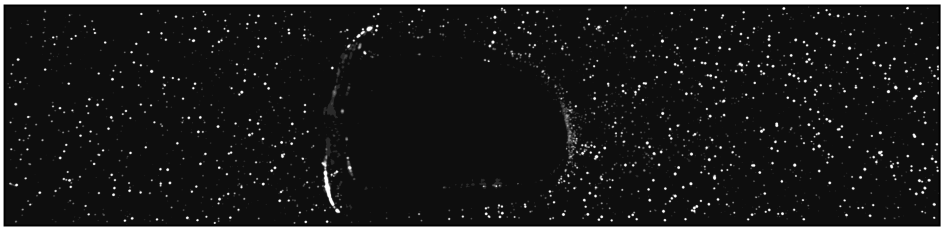

Figure 3: PIV-LIF image of the Taylor Bubble.

We have developed two algorithms to define the bubble shape and the position of bubble trailing edge and bubble nose in each image.

3.1 Summation algorithm

```
procedure SUMMATION(Images, N_1, N_2, R)
    for Every image do
        Summation over N_1 images
        for Every pixel in summed images do
            if Luminosity higher than threshold then
                This and R surrounding pixels are not a bubble
    for Every New Masked Image do
        Average spanwise luminosity over N_2 streamwise length.
        Find maximum (bubble trailing edge) and second maximum (bubble nose) of the derrivative of the average luminosity
```

First step of the summation algorithm is to make the density of the seeding particles in an image larger. As the seeding particles move with larger velocity than the bubble it is possible to obtain larger density of the seeding particles with summation of the larger set of images. Threshold brightness is then used to determine which pixels are the seeds and which are the liquid or the bubble. In the next step, around the bright pixels we create a square of length size in masked image. By doing that, we end up with a topologically connected liquid region, which is separated from the gas bubble.

For the determination of the position of bubble nose and trailing we iterate through the ”masked images” and determine the maximum and second maximum change of luminosity. The first one is the position of the bubble trailing edge and the second is the position of the bubble nose. In order to improve the accuracy of the algorithm the threshold luminosity, the number of averaged images, and the radius around each illuminated pixel can be changed.

3.2 Maximum algorithm

```
procedure MAXIMUM(Images, N)
    for Every image do
        Average spanwise luminosity for N streamwise pixels.
        Find maximum of the averaged luminosity
    for Every image do
        for Every pixel from the position of the maximum to the end of the image do
            if Brigtness at the central cross-section is less than threshold then
                The bubble is still present.
                for Every pixel in the spanwise direction do
                    if Brigtness is less than threshold then
                        The bubble is present.
                    else
                        Break
            else
                Break
```

Second developed algorithm is taking advantage of the special properties of the PIV-LIF images of the Taylor bubble. One of such properties is that at the trailing edge of the Taylor bubble there is a higher luminosity. This is due to the fact that the seeds are trapped in the re-circulation region behind the bubble and deposited at the gas-liquid interface. In some cases they might also stick to the interface region. While conducting experiment this is an important aspect as the high density of seeds near the interface region might alter the statistical properties of the interface region, especially the surface tension.

The algorithm firstly averages luminosity in the spanwise direction and then finds its maximum along the streamwise direction.. The highest luminosity usually corresponds to the trailing edge of the bubble (see Figure 4). After obtaining the position of the bubble trailing edge the algorithm finds the bubble nose by walking through the central line of the pipe and looking at the rapid change of the luminosity at the bubble nose. Center intersection is used as the bubble nose is usually axi-symmetric and occupies almost entire cross-section of the pipe. As the images vary significantly the amount of false-positives is significant and therefore the fit function is used to smooth the position of the minimums and maximums. The rest of the bubble is defined by repeating the same procedure in the spanwise direction from bubble trailing edge to bubble nose.

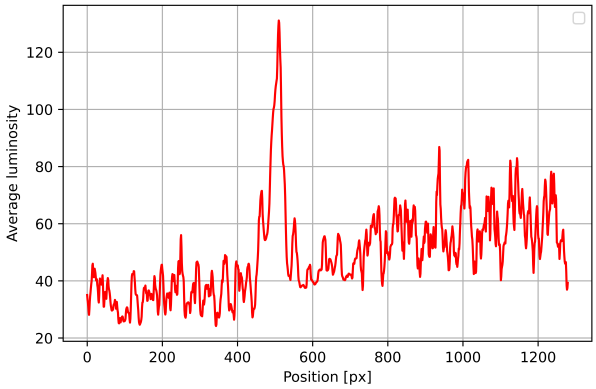

Figure 4: Spanwise-averaged luminosity of PIV-LIF image along the streamwise direction of the Taylor bubble. The highest peak corresponds to the position of the trailing edge of the bubble.

4 RESULTS

The algorithms were tested at two sets of obtained images. The sets differ in bubble sizes and the seeding density.

4.1 Small bubble

For a small bubble both algorithms provide similar results (see Figures 5, 6). The bubble shape is similarly well reconstructed, but the maximum algorithm provides more coherent result. There are still some unconnected regions in the summation reconstruction of the bubble that need to be addressed in further modifications. Maximum algorithm also performs better while determining the positions of the bubble trailing edge and bubble nose regions as the positions obtained from the successive images fluctuate a lot less than for summation algorithm.

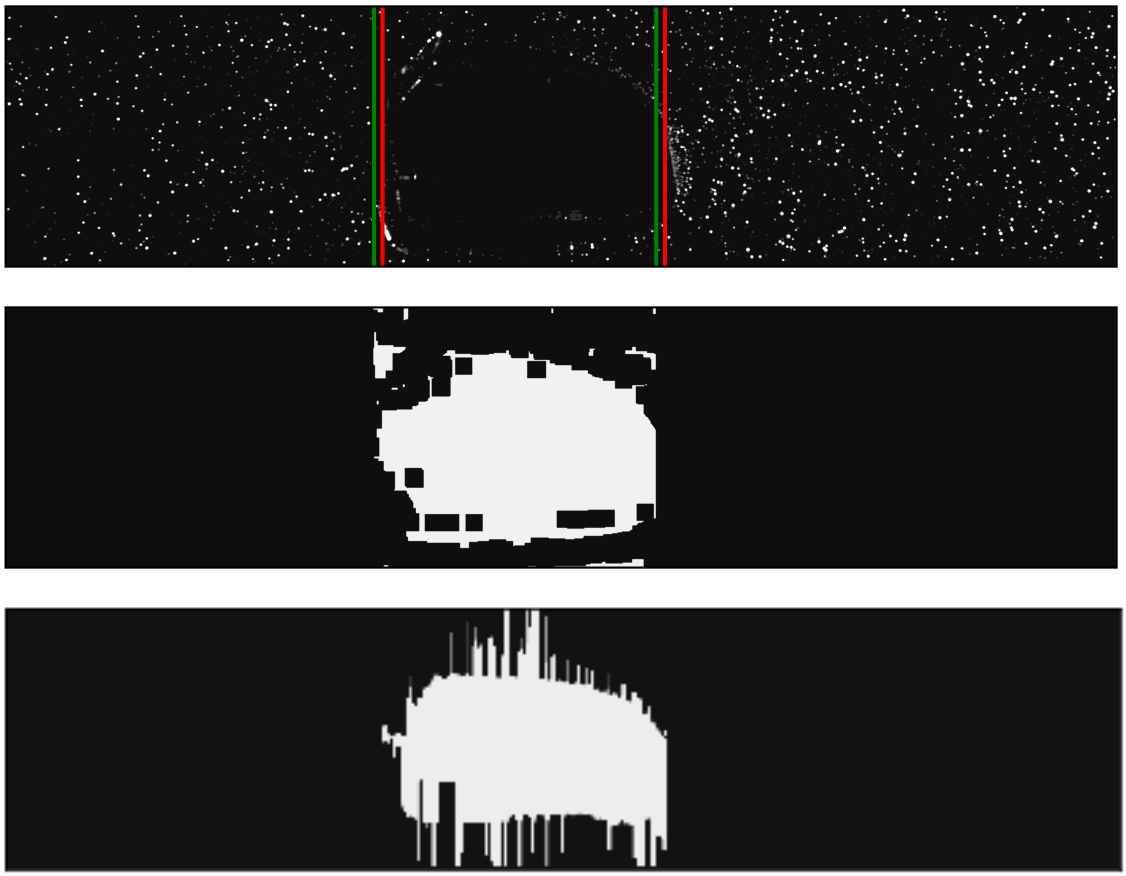

Figure 5: Upper image: PIV-LIF image of the Taylor bubble with the positions of the bubble trailing edge and nose region (Red - Maximum algorithm, Green - Summation algorithm). Middle image: Reconstructed image of a bubble with Summation algorithm. Below image: Reconstructed image of a bubble with Maximum algorithm.

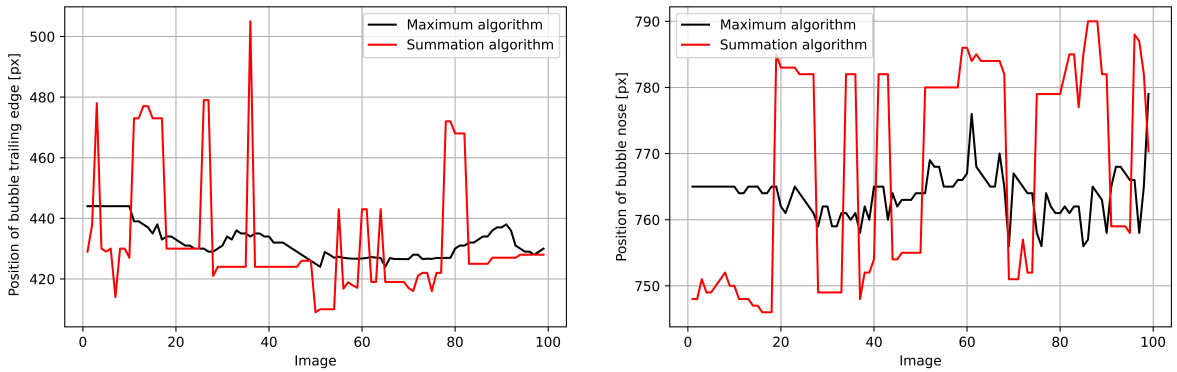

Figure 6: The position of bubble trailing edge (left) and bubble nose (right) determined with different algorithms for small bubble.

4.2 Large bubble

Experimental measurements with large bubble is usually more difficult to perform. This is due to two reasons. Firstly, larger bubbles are more unstable and thus harder to maintain at the constant position. Secondly, the seeding density between the bubble nose and bubble trailing edge regions is usually higher than for smaller bubbles. So, there is significant difference in seeding density between bubble nose and bubble trailing edge regions for larger Taylor bubbles. This is a disadvantage for the maximum algorithm which did not perform good for this set of images. Nevertheless, the summation algorithm performs quite well which is shown in Figures 7 and 8. The bubble is clearly defined and it also captures the positions of bubble trailing edge and nose regions precisely. As the positions of the bubble trailing edge and bubble nose do not fluctuate much through the dataset the algorithm is quite robust.

The largest obstacle is currently the removal of the reflection light inside of the bubble. This can be seen both in Figures 7 and 8. These reflected pixels still have high luminosity and are therefore hard to distinguish from the rest of the signal. This problem needs to be addressed in the future.

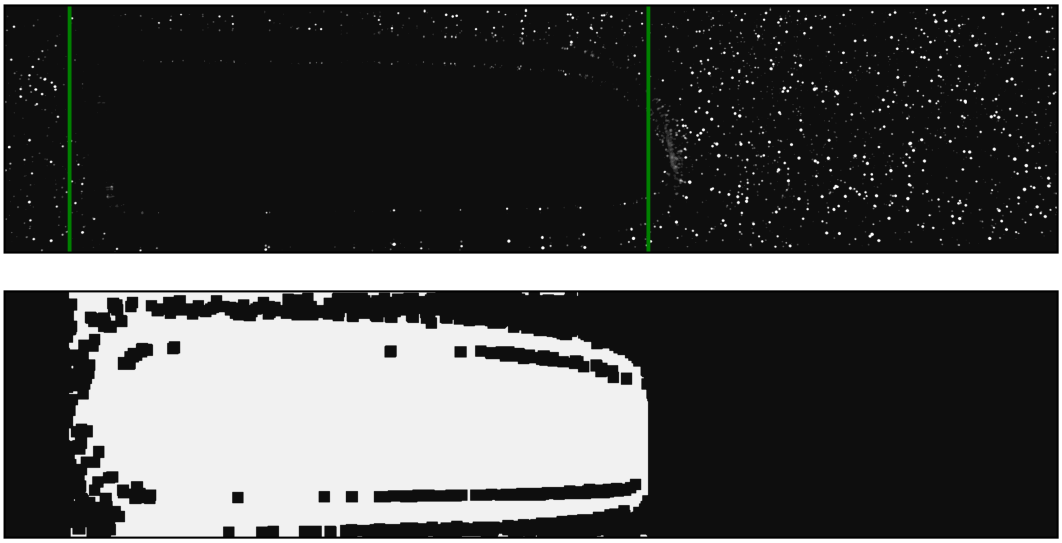

Figure 7: Upper image: PIV-LIF image of the Taylor bubble with the positions of the bubble trailing edge and nose region. Below image: Reconstructed image of a bubble with summation algorithm.

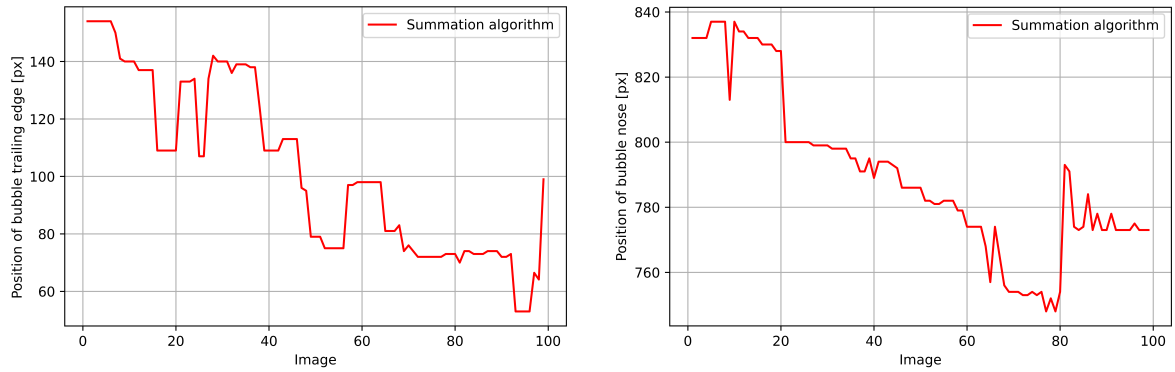

Figure 8: The position of bubble trailing edge (left) and bubble nose (right) determined with summation algorithm for large bubble.

5 CONCLUSIONS

Two algorithms for tracking large interfaces in the PIV-LIF images of the two-phase flows have been developed. Summation algorithm takes advantage of large seeding density of the images and creates a mask around the particles with larger luminosity. Maximum algorithm is based on the larger seeding density at the bubble trailing edge and bubble nose region.

Algorithms have two objectives - to determine the positions of bubble nose and trailing edge and to reconstruct the bubble shape. The first objective was successfully achieved for both algorithms, however the summation algorithm is more robust as it is less settings-dependent. The bubble shape was not sufficiently accurate reconstructed with either of the two algorithms. Therefore further developments of the algorithms will be needed. In order to obtain more accurate results machine learning algorithms will be implemented and tested in our future work.

Code written in Python programming language and small dataset to test the algorithms can be found at:
`https://repo.ijs.si/kren/large-interface-tracking-algorithm`

ACKNOWLEDGMENTS

The authors gratefully acknowledge financial support provided by Slovenian Research Agency, grant for Young Researcher Jan Kren.

REFERENCES

[1] A.O. Morgado, J.M. Miranda and J.D.P. Araújo, J.B.L.M. Campos, ”Review on vertical gas–liquid slug flow”, International Journal of Multiphase Flow, 85, 2016, pp. 348-368.

[2] S. Bennattalah, F. Aloui, M. Souhar, ”Experimental Analysis on the Counter-Current Dumitrescu- Taylor Bubble Flow in a Smooth Vertical Conduct of Small Diameter”, Journal of Applied Fluid Mechanics, 4, 2011, pp. 1-14

[3] E.M.A. Frederix, B. Mikuž, E.M.J. Komen, I. Tiselj, ”LES of a Taylor Bubble in Cocurrent Turbulent Pipe Flow”, 105, 2020, pp. 471-495.

[4] D.T. Dumitrescu, ”Strömung an einer Luftblase im senkrechten Rohr”, ZAMM - Journal of Applied Mathematics and Mechanics / Zeitschrift für Angewandte Mathematik und Mechanik, 23, 1943, pp. 139-149.

[5] B. Mikuž, J. Kamnikar, J. Prošek, I. Tiselj, ”Experimental observation of Taylor bubble disintegration in turbulent flow”, Proc. 28th Int. Conf. Nuclear Energy for New Europe, Portorož, Slovenia, Nuclear Society of Slovenia, September 9-12, 2019, pp. 1-8

[6] LaVision GmbH, ”Particle Image Velocimetry with Laser Induced Fluorescence”, 2021, `http://www.lavision.de/en/techniques/lif-plif/index.php`, Accessed: 2021-07-29

[7] B. Mikuž, E.M.A. Frederix, E.M.J. Komen, I. Tiselj, ”Taylor bubble behaviour in turbulent flow regime”, Proc. Computational Fluid Dynamics for Nuclear Reactor Safety (CFD4NRS-8), Online conference, OECD-NEA, November 25-27, 2020, pp. 1-12

[8] M. Raffel, C. Willert, J. Kompenhans, ”Particle Image Velocimetry: A Practical Guide”, Springer, 1998, pp. 30-120.